

Transcriptomic “portraits” of canine mammary cancer cell lines with various phenotypes

M. Król¹, K.M. Pawłowski¹, J. Skierski², P. Turowski³, A. Majewska¹, J. Polańska⁴, M. Ugorski^{5,6}, R.E. Morty³, T. Motyl¹

¹ Department of Physiological Sciences, Faculty of Veterinary Medicine, Warsaw University of Life Sciences (SGGW), Warsaw, Poland

² Cell Biology Department, National Medicines Institute, Warsaw, Poland

³ Department of Internal Medicine, University of Giessen Lung Center, Justus Liebig University, Giessen, Germany

⁴ Department and Clinic of Obstetrics, Ruminant Diseases and Animal Health Care, Wrocław University of Environmental and Life Sciences, Wrocław, Poland

⁵ Department of Biochemistry, Pharmacology and Toxicology, Wrocław University of Environmental and Life Science, Wrocław, Poland

⁶ Department Immunochemistry, Ludwik Hirszfeld Institute of Immunology and Experimental Therapy, Wrocław, Poland

Abstract. In light of the high incidence of mammary cancer in dogs and completion of the canine genome sequencing, the new possibilities of gene profiling by using DNA microarrays give hope to veterinary oncology. The cell lines isolated from mammary tumors are a valuable tool in developing and testing new pathway-specific cancer therapeutics. Differential cytometric analysis of 6 canine mammary cancer cell lines was performed. We divided cell lines into 3 groups based on their phenotype: 2 lines with high proliferative potential, 2 lines with high antiapoptotic potential, and 2 lines with high metastatic potential. DNA microarray analysis revealed common genes for cell lines of each group. We found that genes encoding the receptors for growth hormone and ghrelin are related to high proliferation rate, while *ABR* (active *BCR*-related) and *TMD1* (TM2 domain containing 1) genes are related to a high antiapoptotic potential of the cancer cells. Metastatic properties of mammary cancer cells seem to be associated with elevated expression of *PGP* (P glycoprotein), *SEMA3B* (semaphorin 3B), and *STIM1* (stromal interaction molecule 1).

Keywords: canine mammary cancer cells, DNA microarray, transcriptomics.

Introduction

DNA microarrays are a powerful modern tool for exploring the biological processes of cells. They are used in large-scale studies of gene expression, called “transcriptional profiling”. This method can be used to find specific gene groups that are expressed differentially in examined tissues when compared to a control sample. The hope of functional genomics is to find new cancer markers, markers of clinical outcome, targets for anticancer therapy, and to explore cancer biology deeper (Król et al. 2009a; Król et al. 2009b). Transcriptomics may be useful for improving

classification of cancer into subgroups, which is not possible when using other methods (Macoska et al. 2002; Ramaswamy et al. 2002).

With the completion of the canine genome sequencing, a powerful research resource has been made available (Lindblad-Toh et al. 2005). In light of the high incidence of mammary cancer in dogs, the cell lines isolated from mammary tumors are a valuable tool in developing and testing new pathway-specific cancer therapeutics. The relevance of using cell lines as a model for canine mammary cancer experiments is supported by results of our previous studies (Pawłowski et al. 2009), showing that gene expression in cell lines isolated from pri-

Received: June 8, 2009. Revised: October 20, 2009. Accepted: December 16, 2009.

Correspondence: T. Motyl, Department of Physiological Sciences, Faculty of Veterinary Medicine, Warsaw University of Life Sciences (SGGW), Nowoursynowska 159, 02-776 Warsaw, Poland; e-mail: tomasz_motyl@sggw.pl

mary tumors can reflect the transcriptome of the tissue of their origin. There is limited information in the literature on gene profiling in canine mammary cancer (Rao et al. 2008; Król et al. 2009c, d; Pawłowski et al. 2009; Rao et al. 2009).

The aim of this study was to find genes and cellular pathways responsible for high proliferative and antiapoptotic potential, as well as cancer cell migration from primary tumor (especially to the lungs). Six canine mammary cancer cell lines (3 adenocarcinomas with various phenotypes, 1 carcinoma, 1 anaplastic cancer, and 1 spindle-cell tumor) were subjects of differential cytometric analysis. Adenocarcinomas constituted half of all the examined cell lines because, biologically, this kind of cancer has almost a 50% chance of developing into a malignant mammary gland tumor (Misdorp 2002). Less frequent are carcinomas (16%), anaplastic cancers (4%), or spindle-cell tumors (Sobczak-Filipiak et al. 2005; Madej and Rotkiewicz 2006).

Our analysis of cell lines with flow and scanning cytometry showed significant differences in their phenotype. Based on the cytometric evaluation and medical history, these cell lines were divided into 3 specific groups with different phenotypes. (The cell lines were not divided morphologically.) The study was focused on finding the common up-regulated genes for cell lines of each group. These genes may be involved in specific biological processes (linked to the phenotype), but are not linked with cell type.

Materials and methods

Media, reagents, glassware, and plastics

Phosphate buffer saline, pH 7.4 (PBS), penicillin-streptomycin, fungizone, and fetal bovine serum (FBS) were obtained from Gibco BRL (Gaithersburg, MD, USA), while acridine orange and DAPI were obtained from Invitrogen (USA). Monoclonal antibodies against Bcl-2 were supplied by Dako Cytomation (Denemark). RPMI 1640 medium, 7 amino-actinomycin D (7AAD), camptothecin (CPT), vinblastine, ribonuclease A, and all the other reagents were obtained from Sigma Aldrich (St. Louis, MO, USA), whereas the Ki-67 detection kit was obtained from Becton Dickinson (USA).

Sterile conical flasks, 4- and 8-chamber culture slides (Lab-Tek), 6-chamber culture plates, sterile

cell scrapers, and sterile disposable pipettes were purchased from Nunc Inc. (Naperville, IL, USA).

Cell lines and cell culture

Three cell lines used in this study were isolated by authors from various mammary adenocarcinomas (PL-20, CMT-W1, CMT-W2), while one cell line was isolated from canine mammary anaplastic cancer (P114) and kindly provided by Dr Gerard Rutteman from Utrecht University in the Netherlands. Two canine cancer cell lines were isolated and kindly provided by Dr Eva Hellmen from Uppsala University (Sweden): mammary carcinoma (CMT-U27) and spindle-cell mammary tumor (CMT-U309). The origin of cell lines CMT-U27, CMT-U309 and P114 was confirmed previously and these cell lines have been described by other authors (Hellmen et al. 1992, 2000; Rao et al. 2008; Spee et al. 2006) and our research team (Król et al. 2009c, Król et al. 2010). The origin of cell lines CMT-W1, CMT-W2 and PL-20 was confirmed by immunohistochemical methods at our Faculty (unpubl. data). The cell lines isolated from tumor samples and paraffin tumor tissue samples were stained with hematoxylin-eosin and antibodies against Ki-67, cytokeratin, vimentin, muscle actin, S100, and p63 proteins. The standard procedure of staining was performed according to the manufacturer's recommendations. The pathological and immunohistochemical examinations were performed by a veterinary pathologist, basing on the WHO and Misdorp (2002) classification.

Cells were cultured in optimum conditions: a medium (RPMI-1640) enriched with 10% (v/v) heat-inactivated FBS, penicillin-streptomycin (50 iU mL⁻¹), and fungizone (2.5 mg mL⁻¹), in an atmosphere of 5% CO₂ and 95% humidified air at 37°C, and routinely subcultured every second day. The methods of canine mammary cancer cells culturing were described previously (Król et al. 2009c, Król et al. 2010).

Induction of apoptosis and immunofluorescent staining for cytometry

The test of cell culture exposure to camptothecin (CPT) was applied to examine cell susceptibility to apoptosis. CPT is an inhibitor of DNA topoisomerase I and is used as an anticancer drug. This method and CPT doses were described in our previous studies (Król et al. 2009c, Król et al. 2010).

Exponentially growing cells were seeded on Lab-Tek 4-chamber culture slides and cultured for 24 h. For apoptosis induction, the medium was then removed and replaced with a medium containing $0.3 \mu\text{g mL}^{-1}$ CPT for 1, 6, 9, and 12 h (cells cultured in 10% FBS medium without CPT were used as a control; 4 replicates were performed).

Cells were fixed in 0.25% formaldehyde for 15 min, washed twice with PBS, suspended in ice-cold 70% methanol, and maintained at 4°C for 30 min. Finally, the methanol was aspirated and samples were stored at -80°C until staining. For antiapoptotic potential measurement, cells were washed twice with PBS and incubated in the dark for 30 min with FITC-conjugated anti-Bcl-2 antibodies diluted 1:100 with PBS. The Bcl-2 protein is commonly known as the main antiapoptotic factor, and its over-expression in cancer cells ensures resistance to chemotherapy. The Bcl-2 content was compared in all examined cancer cell lines, using FITC-conjugated anti-Bcl-2 antibody and counting mean Bcl-2-related fluorescence in a Scan^R screening station. After incubation the cells were washed twice with PBS and then incubated with a $5 \mu\text{g mL}^{-1}$ solution of 7-aminoactinomycin D (7AAD) in PBS containing 2% FCS, 0.1% sodium azide, and 0.3% saponin for 10 min in the dark, to counterstain the DNA. Coverslips were mounted on microscope slides in ICN mounting medium (ICN Biomedicals Inc, Aurora, OH, USA).

Cytometry

The slides were examined using an Olympus Scan^R screening station (Olympus Optical Co., Hamburg, Germany), the modular microscope-based imaging platform designed for fully automated image acquisition and data analysis of biological samples and analysis software (Olympus Scan^R software for screening applications). The number of apoptotic cells and the number of cells in each phase of the cell cycle were examined based on the cytograms. Simultaneous visualization of each cell ensured the proper classification (DNA content and morphology). Scan^R analysis was also performed to measure Bcl-2-related fluorescence. Digital images were processed using Adobe Photoshop software.

The results were analyzed using Microsoft Excel 2003 software (Microsoft Corporation, Redmond, WA, USA) and Prism version 3.00 software (GraphPad Software, San Diego, CA, USA).

DNA ploidy analysis

The DNA ploidy analysis has been described in detail by Darzynkiewicz et al. (1994). The canine mammary tumor cells were stained with DAPI. Canine lymphocytes were used as an external DNA standard and run in parallel with the sample. 10^5 cell nuclei were analyzed in each sample with a FACSC Vantage flow cytometer (Becton Dickinson Sunnyvale, CA). The DNA index (DI) is a value given to express the amount of DNA content relative to normal and is calculated by the following formula:

$$\text{DI} = \frac{\text{mean or modal channel no. of DNA aneuploid } G_0G_1 \text{ peak}}{\text{mean or modal channel no. of DNA diploid } G_0G_1 \text{ peak}}$$

A DNA diploid population (G_0/G_1) is given a DI of $1.00 \pm 10\%$ by definition. Amounts of DNA greater than $2n$ are termed "DNA hyperdiploid" or "hyperploidy".

Growth rate

Exponentially growing cells were seeded on 6-chamber culture plates and cultured for 24 h. To prolong the mitotic phase of the cell cycle, the medium was removed and replaced with a medium containing $0.05 \mu\text{g mL}^{-1}$ of vinblastine (Sigma, USA). Cells were incubated for 1, 2, 3, 4, and 5 h (with 4 replicates). After removal with trypsin-EDTA, the cells were incubated with ribonuclease A (Sigma, USA), and DNA was stained with acridine orange (Invitrogen, USA). The mitotic index (MI) was estimated with FACS Vantage (Becton Dickinson Sunnyvale, CA) flow cytometer (Darzynkiewicz et al., 1994). Coefficient of variation was $<5\%$. The graph was obtained by plotting the logarithm of the mitotic index ($1 + \text{mitotic index}$) versus time of cell incubation in vinblastine. Doubling time (T_d) was calculated by the following formula:

$$T_d = \log_2 a, \text{ where } a \text{ is the graph variable: } y = ax + b.$$

Ki-67 detection

Cell lines CMT-W1 and CMT-W2 are vinblastine-resistant because of P-glycoprotein (PGP) over-expression (this was also detected in the microarray experiment, see the following paragraphs). The assessment of T_d by using the methods described in the previous paragraph was impossible. To decrease the PGP function and sensitize the cells to vinblastine action, the commonly known inhibitors were used: verapamil and

cyclosporine A. Cyclosporine A caused no effect on PGP inhibition, but 2.5 μmol verapamil was added 2 h before vinblastine, and was sufficient to inhibit PGP function in cell line CMT-W2. This allowed us to assess the T_d of CMT-W2, but CMT-W1 remained vinblastine-resistant. Nevertheless, to assess the proliferative potential of this cell line, another method was used. The expression of nuclear antigen Ki-67 was measured. Ki-67 is an antigen expressed only by cells that are active in the cell cycle (in each phase except G_0). After fixation in alcohol, cells were incubated with antibodies against Ki-67 and controlled isotype immunoglobulins. Nuclei were stained with propidium iodide (PI) (Sigma) according to the manufacturer's protocol. The cells were examined in FACS Calibur (Becton Dickinson). Coefficient of variation was $<5\%$.

RNA isolation and validation

P114, CMT-U27, PL-20, CMT-W1, CMT-W2 and CMT-U309 cells were cultured until 90% confluence. The medium was next removed and replaced with PBS. Cells were scraped and the total RNA from the cell suspension samples was isolated using a Total RNA kit (A&A Biotechnology, Poland) according to the manufacturer's protocol. Isolated RNA samples were dissolved in RNase-free water. The quantity of isolated RNA was measured using NanoDrop (NanoDrop Technologies, USA). The samples with adequate amounts of RNA were treated with DNaseI to eliminate DNA contamination. The samples were subsequently purified using RNeasy MiniElute Cleanup Kit (QIAGEN, Germany). Finally RNA samples were analyzed on a BioAnalyzer (Agilent, USA) to measure final RNA quality and integrity. Equal amounts of RNA isolated from all examined cell lines were pooled and used as an experiment control. The RNA pool is widely used as a control in microarray experiments (Sterrenburg et al, 2002). The obvious theoretical advantages of such designs have been established previously (Kendzioriski 2003, 2005; Allison et al. 2002). By using RNA pooling, collected from all of the experimental samples, it is possible to identify correct spots for further analysis (Eisen et al. 1998; Veer et al. 2002). This method also provides an average control for all examined samples.

Probe labeling and hybridization

For each microarray slide, total RNA (10 μg) of each cell line was reverse-transcribed using SuperScript Plus Direct cDNA Labeling System

(Invitrogen, USA) according to the manufacturer's protocol. Single-strand cDNA were stained with Alexa 647 and Alexa 555 (Invitrogen). The efficiency of dye incorporation was measured using NanoDrop (NanoDrop Technologies, USA). For each slide, the RNA of cells from a different passage was used.

Before hybridization, dog-specific oligonucleotide microarray slides *Canis familiaris* V1.0.1 AROS (Operon, USA) with 25 383 probes were prepared according to the manufacturer's protocol. The hybridization mixture contained hybridization buffer (Agilent, USA) and the same amount of stained nucleic acids as that in the examined cell line and pool, which served as a control. Two replicates were performed (dye-swap). Hybridization was performed using automatic hybridization station HybArray12 (PerkinElmer, USA).

Hybridization signal detection, quantification, and analysis

Acquisition and analysis of hybridization intensities were performed using microarray scanner ScanArray HT and ScanExpress software (PerkinElmer, USA). Different types of values were obtained for quantification of the dot intensity. Due to experimental variations in specific activity of oligo-nucleotide target preparations or exposure time that might alter the signal intensity, hybridization data were automatically normalized (LOWESS method) (Oshlack et al. 2007) by ScanExpress software. The average ratio of 3 slides was calculated.

Real-time PCR

Primers (Table 1) were designed using PRIMER3 software (free on-line access). The *HPRT* gene was used as the non-regulated reference gene for normalization of target gene expression (Brinkhof et al. 2006; Etschmann et al. 2006). Quantitative real-time PCR (qRT-PCR) was performed using fluorogenic SYBR Green and the Sequence Detection System Fast 7500 (Applied Biosystems). Data analysis was carried out using the 7500 Fast System SDS Software Version 1.4.0.25 (Applied Biosystems). Relative transcript abundance of a gene is expressed as ΔCt values ($\Delta\text{Ct} = \text{Ct}^{\text{reference}} - \text{Ct}^{\text{target}}$). Relative changes in transcript are expressed as $\Delta\Delta\text{Ct}$ values ($\Delta\Delta\text{Ct} = \Delta\text{Ct}^{\text{pool}} - \Delta\text{Ct}^{\text{examined line}}$). The fold change in expression of the target gene was estimated as $2^{\Delta\Delta\text{Ct}}$. Estimated

Table 1. Primers used in this study.

Target gene	Forward primer	Reverse primer	Optimum annealing	
			temp. (°C)	time (s)
HPRT	AGCTTGCTGGTGAAAAGGAC	TTATAGTCAAGGGCATATCC	59	5
GSK3A	CTCGTCCATTGATGTGTGGTCAG	TACCCAGCACCTTGATGATCTCC	59	5
RPS6KB1	GCACAGCAAATCCTCAGACACCT	GTTCCGGCTGTCGTATTGGAAGTG	59	5
CDC14A	CTCGACTGTTTGCAGGGAATCAGA	CTGGAACAATCCAGTTGAAAGTCA	59	5
ABR	TCAAGTTCACCAGCAGGGAGTTC	ACGATGTAGGGCACCTTGATCT	59	5

fold change for each gene was compared with the same estimation from the microarray analysis.

Statistical analysis

Results were statistically analyzed using the ANOVA and Tukey multiple range tests and Student *t*-test with Prism 3.00 software (GraphPad Software, USA) and Microsoft Excel (USA). Differences were regarded as significant at $P \leq 0.05$.

The microarray data was analyzed with SAM software (Statistical Analysis of Microarrays; Stanford University, USA). The list of genes significantly differing in expression was generated with a false discovery rate (FDR) of $<5\%$, which is sufficient for a reliable microarray analysis (Tuscher et al. 2001; Rao et al. 2008; Rao et al. 2009). To perform further analysis, we chose genes in which expression changed at least 1.3-fold in each of 3 examined slides, and we identified the gene function by using the NCBI database, PANTHER pathway analysis software (Misher et al. 2005) and Architect Pathway software (Stratagene, USA).

Table 2. Cell cycle length (i.e. doubling time T_d) and mean numbers of cells in phases G₁, S, G₂M and of apoptotic cells (A) in cell lines P114, CMT-U27, CMT-W2, CMT-U309, PL-20 and CMT-W1

Cell line	Cell cycle length (h)	Mean number of cells (%)			
		G ₁	S	G ₂ M	A
P114	26.9	64.8	9.9	16.0	9.4
CMT-U27	54.7	64.0	15.0	20.0	1.0
CMT-W2	88.5	59.3	7.0	26.0	6.0
CMT-U309	103.8	61.0	17.0	16.0	6.0
PL-20	158.0	84.0	4.9	7.9	3.2
CMT-W1	no data	52.9	14.2	27.3	5.7

Results

Analysis of ploidy, cell cycle, and apoptosis

Examination of ploidy (Figure 1) revealed that 2 cell lines were diploid (CMT-U27 and CMT-U309), one cell line was tetraploid ($4n$; CMT-W2), whereas the other cell lines were aneuploids: PL-20 was $3n$, P114 was $6n$, and CMT-W1 was $7.5n$. Cytometric analysis revealed significant differences in proliferation rate and apoptosis between examined cell lines (Table 2). Proliferative potential was the highest in P114 ($T_d = 26.9$ h). Cell line CMT-U27 also had a very high proliferative potential ($T_d = 54.7$ h), whereas PL-20 had the longest cell cycle ($T_d = 158$ h). It was impossible to assess the T_d of cell line CMT-W1 because these cells were vinblastine-resistant (because of PGP over-expression) and insensitive to verapamil and cyclosporine A. Cell line CMT-W2 was also vinblastine-resistant, but the action of PGP was inhibited by verapamil. The Ki-67 antigen expression was examined as a parameter of cell proliferation, to assess the percentage of cells remaining active in the cell cycle. This study showed that $94.2\% (\pm 0.4\%)$ of CMT-W1 cells were active in the cell cycle, whereas in cell line CMT-W2 only $83.9\% (\pm 3.9\%)$ of cells showed the Ki-67 expression. These values are representative for 3 independent experiments (Figure 2). Cell line CMT-W1 had 10% higher proliferative potential than CMT-W2.

The cell cycle evaluation (Table 2) showed that in all examined cell lines the highest number of cells remained in the G₁ phase. The cells were examined at 80% confluence to prevent the contact growth inhibition. The number of cells undergoing spontaneous apoptosis differed between the examined cell lines (Table 2). In cell line CMT-U27 (with a high proliferative potential), only 1% of cells undergo spontaneous apoptosis, whereas in cell line P114 (with short T_d) as much as 9.4% of cells are apoptotic.

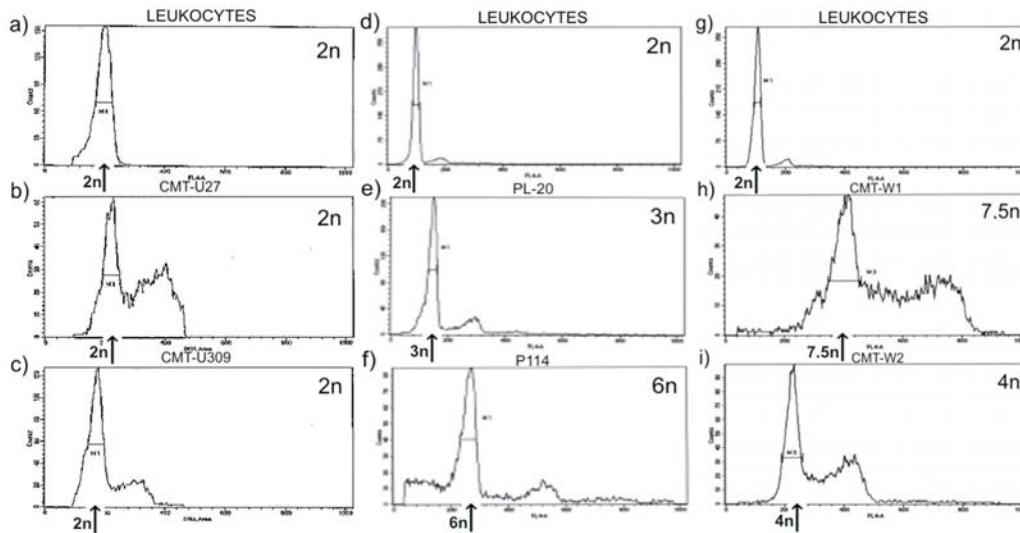


Figure 1. Comparison of histograms used to establish DNA ploidy of the examined cell lines: leukocytes (a, d, g), CMT-U27 cells (b), CMT-U309 cells (c), PL-20 cells (e), P114 cells (f), CMT-W1 cells (h) and CMT-W2 cells (i), representative of 4 independent experiments. Arrows point to G1 peaks.

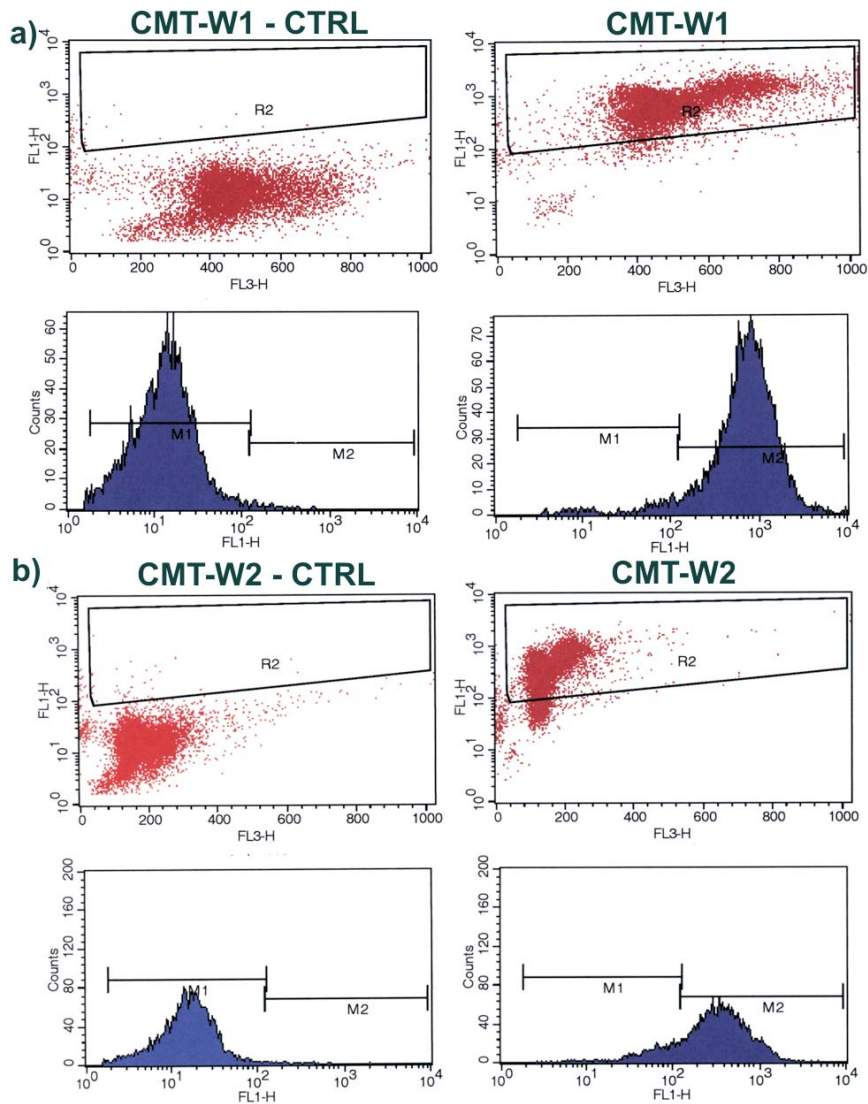


Figure 2. Histograms and cytograms illustrating Ki-67 expression in cell lines CMT-W1 (a) and CMT-W2 (b), representative for 3 independent experiments. Left panel = control cell labeling (Mouse Control Isotype Ig); right panel = examined cells labeled with Ki-67 antibodies.

Expression of Bcl-2 and susceptibility to CPT-induced apoptosis

The Bcl-2 histograms clearly show higher Bcl-2-related fluorescence in both cell lines with lower spontaneous apoptosis (Figure 3, Table 2), (140 U.fl. in CMT-U27 and 106 U.fl. in PL-20). The mean fluorescence intensity of Bcl-2 in P114 with the highest number of cells undergoing spontaneous apoptosis was only 50 U.fl.

CPT induced a progressive, significant increase in apoptotic cell number in each cell line,

especially in P114 with the lowest Bcl-2 expression. In this cell line the number of apoptotic cells after 12 h of incubation with CPT increased to 29.8% (Figure 4). The lowest response to CPT was observed in CMT-U27 cells with the highest Bcl-2 expression. This experiment was repeated 4 times with the same effect. The number of apoptotic cells in line CMT-U309 increased until the 6th hour of culture exposure to CPT, and significantly decreased thereafter (Figure 4). We assume that this effect was artificial and resulted from

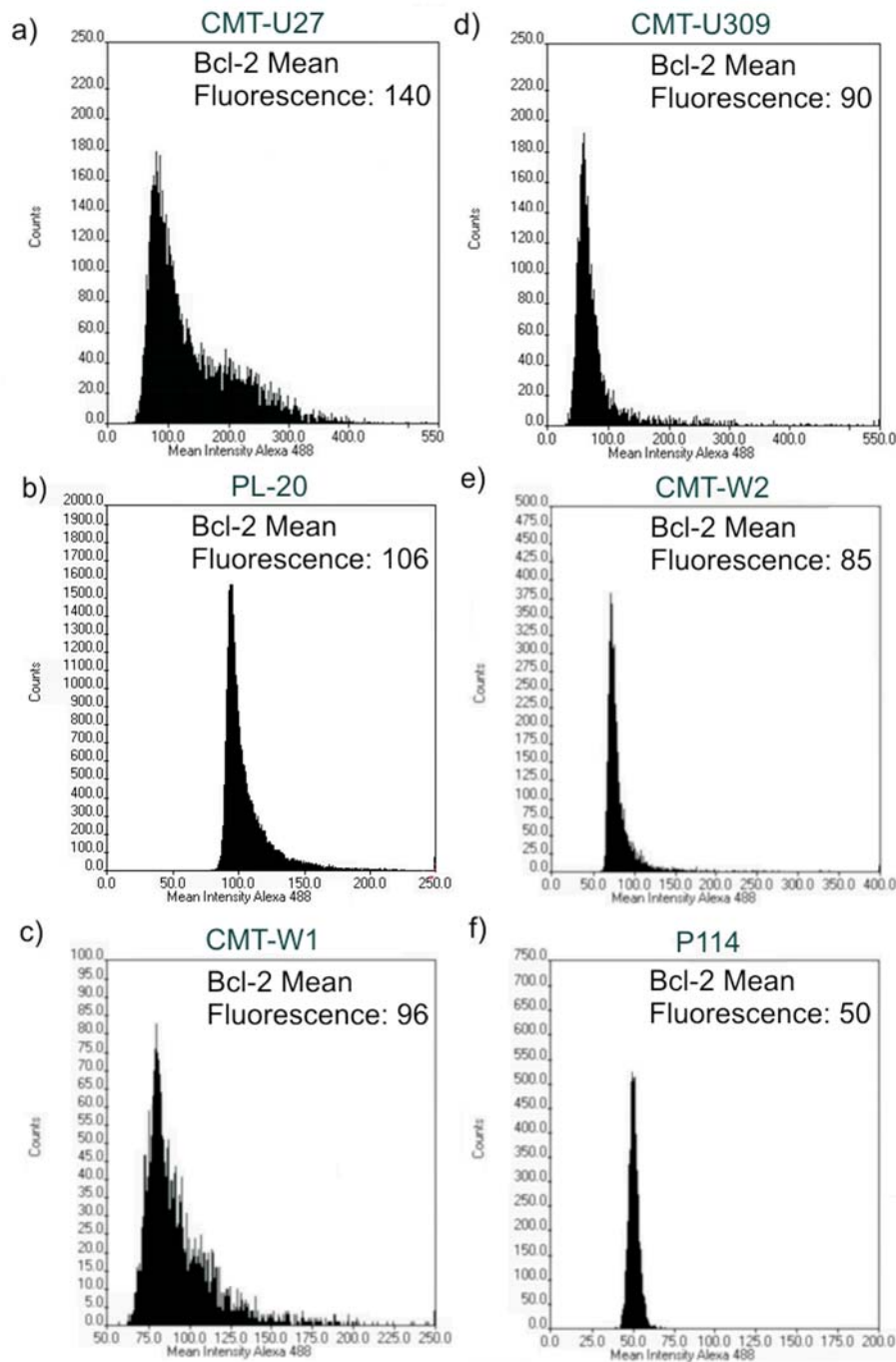


Figure 3. Comparison of histograms of cell lines CMT-U27 (a), PL-20 (b), CMT-W1 (c), CMT-U309 (d), CMT-W2 (e), and P114 (f), labeled with FITC-conjugated anti-Bcl-2 antibody, representative of 4 independent experiments.

Table 3. List of common genes for each phenotype group. Gene name and symbol, biological and molecular process and pathway of gene involvement are listed according to the Panther Database classification (www.pantherdb.org). The analyzed genes were significantly up-regulated at the level of FDR < 5% (SAM software, Stanford University, USA), with fold change >1.3

Phenotype	Gene name and symbol	Molecular function	Biological process	Pathway
1	2	3	4	5
High proliferative potential: lines P114, CMT-U27	GHR, growth hormone receptor	receptor	cell surface receptor mediated signal transduction, intracellular signaling, developmental process	growth hormone signaling
	GHSR, growth hormone secretagogue receptor	G-protein coupled receptor	G-protein mediated signaling	growth hormone signaling
	CDC14A, CDC14 cell division cycle 14 homolog A	protein phosphatase	protein phosphorylation, cell cycle control, mitosis	no data
	GSK3A, glycogen synthase kinase 3 alpha	non-receptor serine/threonine protein kinase	other polysaccharide metabolism; glycogen metabolism; protein phosphorylation, other receptor-mediated signaling pathway, other intracellular signaling cascade, embryogenesis; segment specification, neurogenesis, mesoderm development, mitosis, cell proliferation and differentiation	Ras pathway, PDF signaling pathway, G-protein pathway, Wnt signal. pathway, IGF/Insulin pathway, angiogenesis, interleukin pathway, cadherin and PI3 kinase pathway
High anti-apoptotic potential: lines CMT-U27, PL-20	ABR, active BCR-related	guanyl-nucleotide exchange factor	other intracellular signaling cascade	FGF signaling pathway, angiogenesis
	CAPN9, calpain 9	cysteine protease	proteolysis	Huntington disease (calpain)
	TMD1, TM2 domain containing 1	another function protein	neuronal activities; induction of apoptosis	no data
	GRM4, glutamate receptor, metabotropic 4	G-protein coupled receptor	G-protein mediated signaling; neuronal activities	metabotropic glutamate receptor group III pathway
High metastatic potential: lines CMT-W1, CMT-W2	C19orf6, chromosome 19 open reading frame 6	structural protein	unclassified	no data
	DLST, dihydrolipoamine S-succinyl transferase	acyltransferase	unclassified	no data
	HAL, histidine ammonia-lyase	unclassified	unclassified	no data
	KIF21A, kinesin family member 21A	microtubule binding motor protein	intracellular protein traffic, protein targeting and co-localization, cell structure	no data
	PGP, ATP-binding cassette, subfamily B (MDR/TAP), member 1A	cysteine protease	proteolysis; ligand-mediated signaling	no data
	PHACTR4, phosphatase and actin regulator 4	phosphatase modulator	neuronal activities; cell structure	no data
	SCYL3, SCY1-like 3	unclassified	cell motility	no data
	SEMA3B, sema domain, secreted (semaphorin) 3B	signaling molecule; membrane-bound signaling	receptor protein tyrosine kinase signaling pathway; other receptor mediated signaling pathway, neurogenesis, tumor suppressor	no data
SEPT3, septin 3	cytoskeletal protein, small GTPase	cytokinesis	no data	

Table 3. cont.

1	2	3	4	5
	SMYD1, SET and Mync domain containing 1	transcription cofactor	mRNA transcription regulation, cell proliferation and differentiation	no data
	STIM1, stromal interaction molecule 1	unclassified	unclassified	no data
	TMEM149, transmembrane protein 149	unclassified	unclassified	no data
	WIBG, within bgen homolog	unclassified	unclassified	no data
	YEATS2, YEATS domain containing 2	transcription factor; chromatin/chromatin-binding protein	mRNA transcription	no data

detachment of apoptotic cells and wash-out from the slides in the course of staining procedure. This experiment was repeated 10 times and apoptotic cells detachment was seen on every slide.

The performed cytometric analysis was sufficient to divide the cell lines into 2 groups based on their phenotypic features:

1. Short cell cycle was specific for P114 and CMT-U27, which were qualified as cell lines with high proliferative potential.

2. Based on the results of Bcl-2-related fluorescence measurement and number of apoptotic cells, CMT-U27 and PL-20 were classified as cell lines with high antiapoptotic potential.

Additionally, another (third) phenotype group was discriminated:

3. Medical history of dogs from which cell lines CMT-W1 and CMT-W2 were isolated was sufficient to qualify these cell lines to the group with ability to metastasize to the lungs (primary tumors from which the cells were isolated gave metastases to the lungs). Other cell lines did not give metastases to the lungs.

Cell line CMT-U309 was not assigned to any of the groups. This cell line has medium proliferative and antiapoptotic potential, and lacks medical history regarding its metastases.

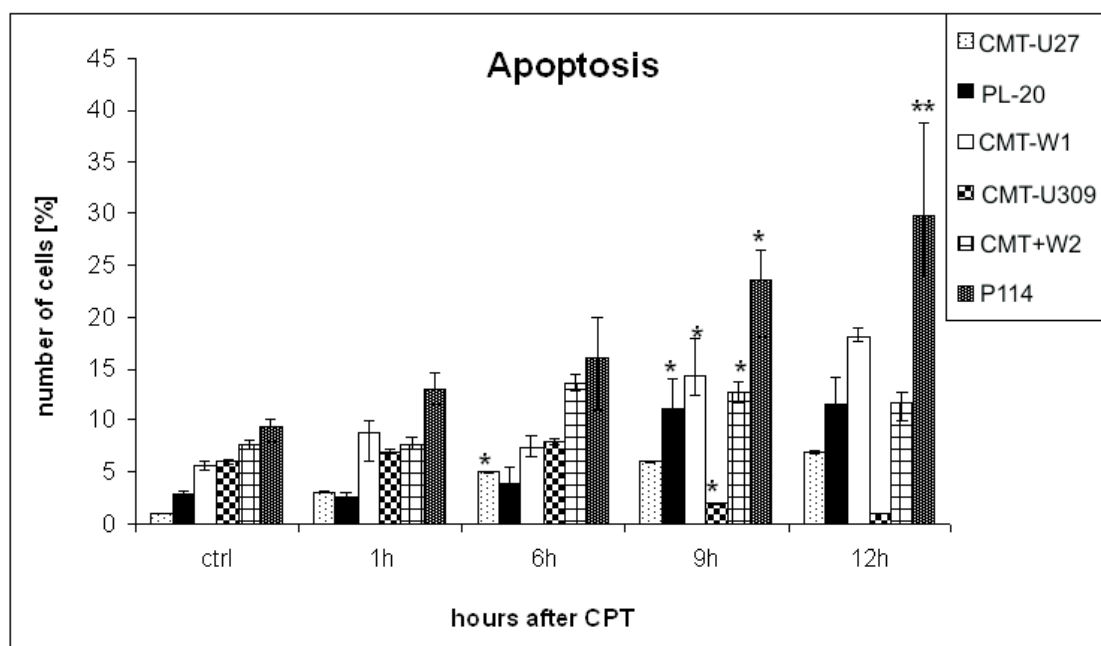


Figure 4. Numbers of apoptotic cells (%) in cell lines CMT-U27, PL-20, CMT-W1, CMT-U309, CMT-W2 and P114 before and 1, 6, 9, and 12 h after camptothecin (CPT) administration ($0.3 \mu\text{g mL}^{-1}$). Results are means \pm SD ($N = 4$).

Significant ($P \leq 0.05$) differences between means at the same time of exposure to CPT are marked with asterisks

Transcriptomic “portraits” of canine mammary cancer cell lines

This study showed 117 significantly up-regulated genes (FDR < 5%) in cell line CMT-U309; 102 in CMT-W2; 89 in P114; 73 in CMT-W1; 63 in CMT-U27; and 54 in PL-20.

Further analysis of up-regulated genes among the groups (Table 3) showed 4 common genes for both cell lines with high proliferative potential (P114 and CMT-U27): *GHR* (growth hormone receptor), *GHSR* (growth hormone secretagogue receptor), *CDC14A* (cell division cycle 14 homolog A), and *GSK3A* (glycogen synthase kinase 3 alpha). Both cell lines with high antiapoptotic potential (CMT-U27 and PL-20) also showed 4 common up-regulated genes (Table 3): *ABR* (active *BCR*-related), *CAPN9* (calpain 9), *TMD1* (TM2 domain containing 1), and *GRM4* (glutamate receptor metabotropic 4). The analysis showed 14 common genes for both cell lines with the ability to metastasize to the lungs (CMT-W1 and CMT-W2): ATP-binding cassette subfamily B (*PGP*), semaphorin 3B (*SEMA3B*), stromal interaction molecule 1 (*STIM1*), chromosome 19 open reading frame 6 (*C19orf6*), dihydro-lipoamine S-succinyl transferase (*DLST*), histidine ammonia-lyase (*HAL*), kinesin family member 21A (*KIF21A*), phosphatase and actin

regulator 4 (*PHACTR4*), SCY1-like 3 (*SCYL3*), septin 3 (*SEPT3*), SET and Mync domain containing 1 (*SMYD1*), transmembrane protein 149 (*TMEM149*), within bgn homolog (*WIBG*), and YEATS domain containing 2 (*YEATS2*).

No one common gene for all 3 adenocarcinomas was found, whereas 14 common genes were found for pairs of adenocarcinomas that belong to the same phenotype group (CMT-W1 and CMT-W2). This indicates that among the up-regulated genes the phenotype-specific genes were found, but not genes that are cell-type linked.

For the purpose of microarray data validation, we have randomly selected 4 genes for qRT-PCR analysis (Figure 5): *ABR* (active *BCR* – related), *RPS6KB1* (ribosomal protein S6 kinase, 70 kDa, polypeptide 1), *CDC14A* (cell division cycle 14 homolog A), *GSK3A* (glycogen synthase kinase 3 alpha). Real-time qRT-PCR results showed similar trends in gene expression changes as those observed in our microarray experiments.

Discussion

So far only several papers describing transcriptional studies in canine mammary gland tumors have been published (Rao et al. 2008; Król et al. 2009a,

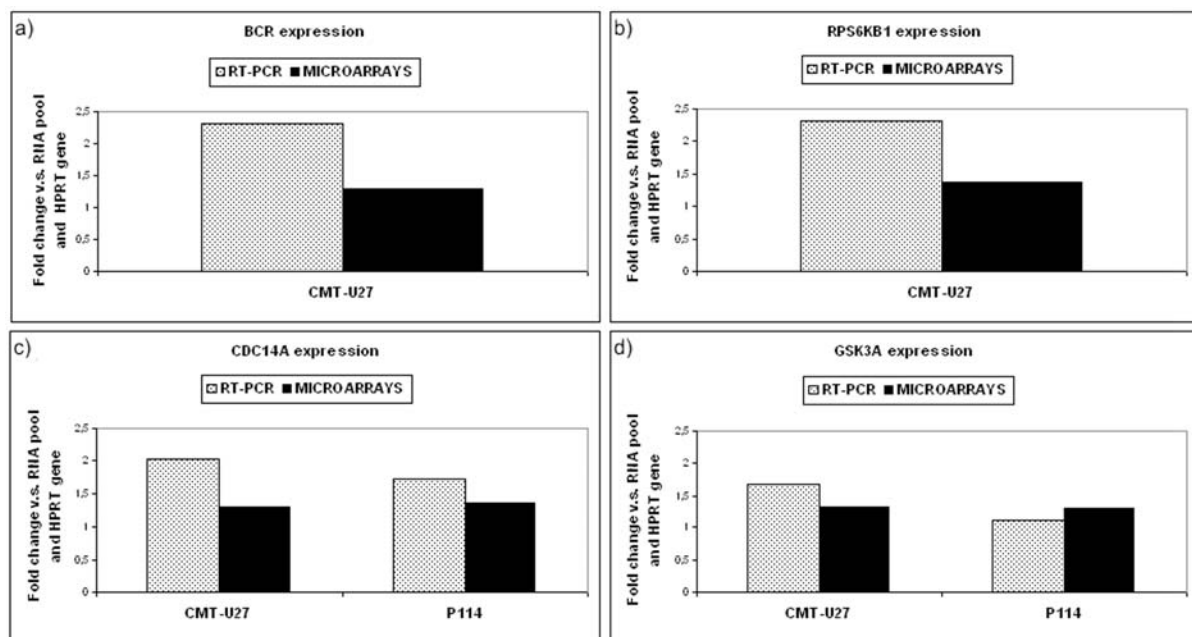


Figure 5. Confirmation of microarray results by qRT-PCR. The fold change detected with qRT-PCR was calculated based on the *HPRT* control gene expression and compared to the expression of all examined cell lines (pooled transcripts). The fold change was significantly different ($P < 0.05$)

b, c; Król et al. 2010; Pawłowski et al. 2009; Rao et al. 2009).

In this study, 3 adenocarcinomas (simple carcinoma, anaplastic cancer, and spindle-cell tumor) were examined and strong differences in their phenotype were noted. Only 2 of them were diploids, while the other 4 cancers were hyperploids (Figure 1), which is typical for the canine mammary tumors. In the examination performed by Rutteman et al. (1988), 61.8% of malignant and 17.4% of non-malignant canine mammary tumors were aneuploids. This indicates that ploidy in mammary tumors in dogs differs from that in human breast cancer, where most of the tumors are diploid. There were also differences in the examined cell lines when assessing cell cycle length, number of cells in the cell cycle, as well as antiapoptotic potential, i.e. number of apoptotic cells after incubation with CPT and Bcl-2-related fluorescence (Figures 3 and 4).

In this study, the transcriptomic profile of each of the 6 cell lines was compared to the pool of all examined cell lines. Gene pools are commonly used as a reference in similar studies (Sterrenburg et al. 2003). In the case of microarray experiments with canine mammary cancer, obtaining an alternative sufficient control other than gene pools is virtually impossible. In dogs, to use the healthy mammary tissue as a control is not a good reference. Dogs have an estrous cycle distinct from other mammals. The hormonal status of each phase of the estrus cycle in the mammary gland of the bitch is very complex (Rao et al. 2008). As a result of the common treatment with progestins and anti-inflammatory steroids (e.g. dexamethasone), the estrus can be followed by a prolonged luteal phase coinciding with high (pregnancy-like) concentrations of progesterone (without subsequent lactation) or the estrus can be “silent” (with no signs). Moreover, mammary cancer due to hormonal activity in the mammary gland is a problem even if the ovaries were removed a few years before. These are the reasons why there is no evidently healthy tissue without strong hormonal influence. Thus, the “healthy” tissue is not a good and authoritative control.

In our previous study (Król et al. 2009c) we compared gene expression of cell lines CMT-U27 and CMT-U309. We concluded that high proliferative and antiapoptotic potential is related to the up-regulation of growth hormone receptor and calmodulins. Higher expression of calmodulins in CMT-U27 than in CMT-U309 was also confirmed at the level of proteins. The current

study confirms our previous results (Król et al. 2009c), showing the growth hormone involvement in a high growth rate of canine mammary cancer cell lines. Analysis of up-regulated genes showed 4 common genes for both cell lines with high proliferative potential: P114 and CMT-U27 (Table 3). These include *GHR* (growth hormone receptor), *GHSR* (growth hormone secretagogue receptor), *GSK3A* (glycogen synthase kinase 3 alpha), and *CDC14A* (cell division cycle 14 homolog A). Higher levels of growth hormone and insulin-like growth factor (IGF-1) in plasma and tissues are risk factors of breast cancer and mammary cancer in mice (Wagner et al. 2006). The effect of growth hormone on the cancer cell proliferation rate is commonly known (Gebre-Medhin et al. 2001). In both cell lines with the shortest cell cycles, an up-regulation of another gene involved in somatotrophic axis was found: *GHSR*. Ghrelin is an internal ligand of growth hormone secretagogue receptor (GHSR), increasing growth hormone secretion (Jeffrey et al. 2005). Ghrelin has been described as a carcinogenic factor in breast cancer by stimulating cell proliferation in autocrine or paracrine mechanism. In 2005, Jeffrey et al. published the first report describing differences in the expression of GHSR between normal breast tissue and tumor. The mechanism underlying ghrelin-induced proliferation in breast cancer is unknown, although it is likely to act by stimulating the mitogen-activated protein kinase pathway. Experimental injection of high doses of ghrelin to patients with hormone-dependent cancers increased tumor proliferation (Chopin et al. 2005). Our own studies showed the involvement of ghrelin in canine mammary adenocarcinoma metastasis to the lungs (Król et al. 2010).

Another up-regulated gene in cell lines P114 and CMT-U27 is *GSK3A*. Ougolkov et al. (2006) described a kind of paradox observed in cancer cells. When focusing on the cellular pathways of growth hormone and ghrelin, it is clear that they inhibit *GSK3B* (its inhibition promotes *GSK3A* activation) and vice versa. However, in neoplastic cells the parallel over-expression of somatotrophic axis-related genes and GSK3 genes is observed, which increases cancer cell proliferation. It is possible that the lack of inhibitory effect of growth hormone and ghrelin on GSK3 (and vice versa) in cancer cells is related to a compensative increase in *GSK3A* expression. This suggests also the existence of a mediating molecule between GSK3 and these pathways, like JUN transcription factor,

which stimulates growth hormone secretion (growth hormone also stimulates JUN). This observation needs further investigation, as the role of GSK3 and cellular interactions in cancer still remains unknown. Another important action of GSK3 is the activation of oncogenic molecule NF-kappaB. It has been shown that inhibition of GSK3 leads to a decrease in NF-kappaB function (Ougolkov et al. 2006). GSK3 through NF-kappaB increases tumor proliferation and seems to be a mutagenic factor. Some authors suggest that GSK3 may become a new target for cancer therapy (Ougolkov et al. 2006).

The next common gene for both cell lines with short T_d (Table 2) is *CDC14A*, which controls the cell cycle and mainly acts in anaphases (D'Amours et al. 2004). The CDC14A protein controls microtubule activation and fiber stabilization. It leads to cell cycle completion.

Analysis of up-regulated genes in both cell lines with high antiapoptotic potential: CMT-U27 and PL-20 (Figures 3 and 4) showed 4 common genes (Table 3): *ABR* (active *BCR*-related), *TMD1* (TM2 domain containing 1), *GRM4* (glutamate receptor metabotropic 4), and *CAPN9* (calpain 9).

Among the listed genes, the most important antiapoptotic factor seems to be the *ABR* (active *BCR* – related) gene, which interacts (through *TP53*, *AR*, *MDM2*, and *STAT1*) with the very important and commonly known gene in breast cancer: *BRCA-1*. *ABR* inhibits DNA repair, thus increasing the possibility of mutation and promoting oncogenesis. It also inhibits the cell cycle. The main function of this gene is inhibition of apoptosis. This function was previously described in leukemias (Keeshan et al. 2001). It increases Bcl-2 and Bcl-xL expression, which are responsible for antiapoptotic effect. Cell lines CMT-U27 and PL-20 showed the highest Bcl-2 expression (Figures 3 and 4).

ABR and *TMD1* (another common up-regulated gene for both CMT-U27 and PL-20) are involved in drug-resistance of tumor cells. *TMD1* encodes the TM domain, a part of ATP-binding cassettes. We assume that co-expression of both listed genes is related to CPT resistance of cell lines CMT-U27 and PL-20 (Figure 4). The number of apoptotic cells after 6 h of CPT incubation in CMT-U27 and PL-20 was comparable with the number of spontaneous apoptotic cells in other cancer lines. It is probable that the long time of CPT exposure (Brinkhof et al. 2006) (9 and 12 h) had broken drug-resistance in these cell lines, or Bcl-2 protein beside apoptosis

may be involved in some pathways of cellular resistance to chemotherapy.

There is currently no information in the literature on the involvement of the other 2 common up-regulated genes in the antiapoptotic process. *CAPN9* is a calcium-related enzyme and its up-regulation confirms our previous study describing the role of calcium (calmodulins) in antiapoptotic potential (Król et al. 2009c).

The possibility that tumor cells migrate from a primary locus to the distal tissues and organs is the main dilemma in oncology. Metastasis is a very complicated process. Thus describing the gene expression profile of metastatic cancer cells is extremely challenging. Analysis of up-regulated genes showed 14 common genes for both cell lines with ability to metastasize to the lungs (CMT-W1 and CMT-W2), (Table 3): *PGP* (ATP-binding cassette subfamily B), *SEMA3B* (semaphorin 3B), *STIMI* (stromal interaction molecule 1), *C19orf6* (chromosome 19 open reading frame 6), *DLST* (dihydrolipoamine S-succinyl transferase), *HAL* (histidine ammonia-lyase), *KIF21A* (kinesin family member 21A), *PHACTR4* (phosphatase and actin regulator 4), *SCYL3* (SCY1 like-3), *SEPT3* (septin 3), *SMYD1* (SET and Mync domain containing 1), *TMEM149* (transmembrane protein 149), *WIBG* (within bgen homolog), and *YEATS2* (YEATS domain containing 2).

There is no clear indication of how *PGP* functions in the metastatic process. *PGP* up-regulation in both metastatic cell lines confirms our cytometric experience with vinblastine-resistance of cell lines CMT-W1 and CMT-W2. Among the 14 up-regulated genes in CMT-W1 and CMT-W2, two widely known genes involved in metastatic process were found: *SEMA3B* and *STIMI*. *SEMA3B* is a very important factor that inhibits cell proliferation but increases cell migration and cancer dissemination. *SEMA3B* acts through MAPK kinase, inducing p21 protein, which inhibits tumor growth. It also activates IL8, which strongly stimulates the metastatic process (Rolny et al. 2008). Although *SEMA3B* inhibits tumor growth, the prognosis in patients with its over-expression is poor because of the high possibility of distal metastases. Over-expression of cell lines *SEMA3B* in MDA-MB435 and A549 leads to skin tumor metastases (Rolny et al. 2008), but intravenous injection of *SEMA3B* to mice did not make any effect. It shows that *SEMA3B* action is mainly involved in tumor cell migration from primary tumor (Christensen et al. 2005). It also plays an important role in changing the tumor's

microenvironment (Donnenberg et al. 2005). The attraction of blood-circulating macrophages to the tumor (tumor-associated macrophages) is a very important process in angiogenesis and cancer development. *SEMA3B* induces IL8 – a chemokine responsible for macrophage migration to the cancer locus (Donnenberg et al. 2005). Macrophages play an important role in tumor development by angiogenesis promotion and lead to extracellular matrix remodeling and degradation, which increase tumor cell migration. Clinical studies show that if there is a higher amount of tumor-associated macrophages in tumor tissue, then the prognosis is poor.

The role of *STIM1* in tumor metastasis to the lungs was described by Suyama et al. (2006). *STIM1* increases cell migration and metastasis to distal organs. More specifically, it inhibits melanoma proliferation and increases its metastatic potential.

Our results show that both *SEMA3B* and *STIM1* can initiate the process of metastasis, but *SEMA3B* plays the most important role. Cell population in the primary tumor is biologically heterogenic, which is an effect of mutations, changes in gene expression, and genetic instability in proliferating cells. During cancer progress the cells become invasive and show a high metastatic potential (Christensen et al. 2005).

Conclusions

On the basis of the cellular pathways and the current literature, we conclude that:

1. The high proliferative potential of canine mammary cancer cells is related to up-regulation of 4 genes (Figure 6), encoding:

a) growth hormone receptor (*GHR*) and growth hormone secretagogue receptor (*GHSR*), both involved in the somatotrophic axis;

b) a kinase that shows oncogenic action through activation of NF-kappaB (*GSK3A*);

c) a cytokine that regulates the cell cycle (*CDC14A*).

2. High antiapoptotic potential of canine mammary cancer cells is related to higher expression of 4 genes (Figure 6): *ABR* (active *BCR*-related), *TMD1* (TM2 domain containing 1), *CAPN9* (calpain 9), and *GRM4* (glutamate receptor metabotropic 4).

3. The ability of cancer cells to metastasize (especially to the lungs) may be related with up-regulation of 14 genes, but few of them are important: *PGP* (P glycoprotein), *SEMA3B* (semaphorin 3B, which changes the tumor microenvironment and produces chemokines), as well as *STIM1* (stroma interaction molecule 1, which increases cell migration and tumor progression in distal organs).

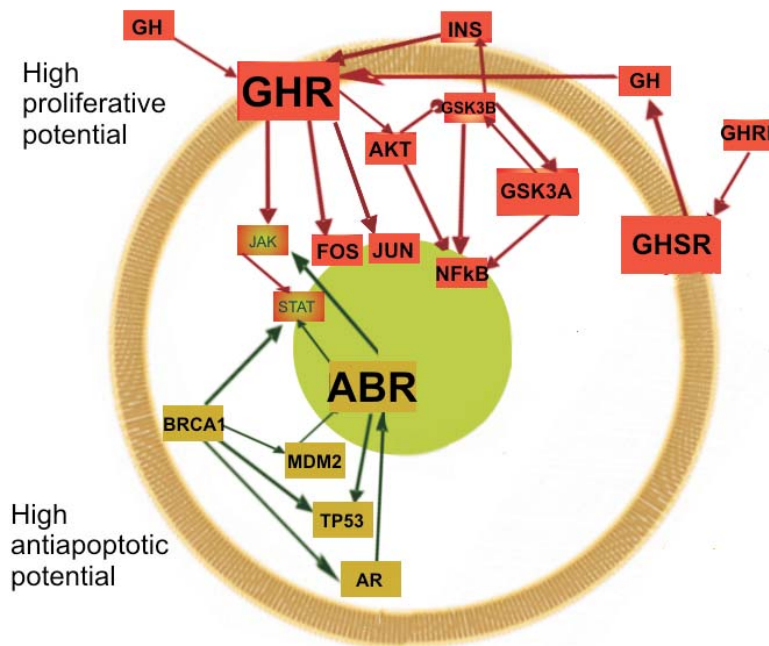


Figure 6. Involvement of up-regulated genes in cell proliferation and resistance to apoptosis. Green circle = nucleus; brown perimeter = cell membrane. AKT = protein kinase B; AR = androgen receptor; ABR = active *BCR* – related; BRCA1 = breast cancer gene 1; GH = growth hormone, GHR = growth hormone receptor; GHSR = growth hormone secretagogue receptor; GHRL = ghrelin; GSK3A/B = glycogen synthase kinase 3 A/B; INS = insulin; MDM2 = mouse double minute 2; NFkB = nuclear factor kappa B; TP53 = tumor protein p53.

Acknowledgements. We thank Dr. Eva Hellmen from Uppsala University for her kind donation of cell lines CMT-U27 and CMT-U309, and Dr. Gerard Rutteman from Utrecht University for his kind donation of cell line P114. We would like to thank Dr. Clifford Meyers and Ms. Victoria Brennan for their contribution to the preparation of the manuscript.

This paper was supported by the Polish Ministry of Science and Higher Education (grant no N308230536), the European Social Fund, State Budget within Integrated Program of Regional Development (2.6. Point „Regional Innovative Strategies and Knowledge Transfer” and “Regional Innovative Strategies and Knowledge Transfer”), a project of the Masovia Region (“Masovia Scholarship for PhD students”), and the Lower Silesia Region budget.

REFERENCES

- Allison DB, 2002. Statistical methods for microarray research for drug target identification. *Proc Soc Stat Sect* 37–44.
- Brinkhof B, Spee B, Rothuizen J, Penning LC, 2006. Development and evaluation of canine reference genes for accurate quantification of gene expression. *Anal Biochem* 356: 36–43.
- Chopin LK, Jeffery PL, Yeh A, McNamara JF, Wight R, Herington AC, 2005. Ghrelin and hormone-dependent cancer. *Proc Aust Physiol Pharmacol Soc*.
- Christensen CN, Ambartsumian G, Gilestro B, et al. 2005. Proteolytic processing converts the repelling signal Sema3E into an inducer of invasive growth and lung metastasis. *Cancer Res* 65: 6167–6177.
- D’Amours D, Amon A, 2004. At the interface between signaling and executing anaphase—Cdc14 and the FEAR network. *Genes Dev* 18: 2581–2595.
- Darzynkiewicz Z, Robinson JP, Crissman HA, 1994. *Methods in cell biology. Flow cytometry*, 2nd ed. Part A. San Diego, California: Academic Press. 41: 211–217, 409–410.
- Donnenberg V, Donnenberg A, 2005. Multiple drug resistance in cancer revisited: the cancer stem cells hypothesis. *J Clin Pathol* 45: 872–877.
- Eisen MB, Spellman PT, Brown PO, Botstein D, 1998. Cluster analysis and display of genome-wide expression patterns. *Proc Natl Acad Sci U S A* 95: 14863–14868.
- Etschmann B, Wilcken B, Stoevesand K, von der Schulenburg A, Sterner-Kock A, 2006. Selection of reference genes for quantitative real-time PCR analysis in canine mammary tumors using the GeNorm algorithm. *Vet Pathol* 43: 934–942.
- Gebre-Medhin M, Kindlom LG, Wennbo H, Tornell J, Meis-Kindblom JM, 2001. Growth hormone receptor is expressed in human breast cancer. *Am J Pathol* 158: 1217–1222.
- Hellmen E, 1992. Characterization of four in vitro established canine mammary carcinoma and one atypical benign mixed tumor cell lines. *In Vitro Cell Dev Biol* 28A: 309–319.
- Hellmen E, Moller M, Blankenstein MA, Andersson L, Westermark B, 2000. Expression of different phenotypes in cell lines from canine mammary spindle-cell tumours and osteosarcomas indicating a pluripotent mammary stem cell origin. *Breast Cancer Res Treat* 61: 197–210.
- Jeffrey PL, Murray RE, Yeh AH, McNamara JF, Duncan RP, Francis GD, et al. 2005. Expression and function of the ghrelin axis, including a novel preproghrelin isoform, in human breast cancer tissues and cell lines. *Endocr Relat Cancer* 12: 839–850.
- Keeshan K, Mills KI, Cotter TG, McKenna SL, 2001. Elevated Bcr-Abl expression levels are sufficient for a haematopoietic cell line to acquire a drug-resistant phenotype. *Leukemia* 15: 1823–1833.
- Kendzierski CM, Zhang Y, Lan H, Attie AD, 2003. The efficiency of pooling mRNA in microarray experiments. *Biostatistics* 4,3: 465–477.
- Kendzierski CM, Irizarry RA, Chen KS, Haag JD, Gould MN, 2005. On the utility of pooling biological samples in microarray experiments. *Proc Natl Acad Sci USA* 102: 124252–124257.
- Król M, Pawłowski KM, Otrębska D, Motyl T, 2009a. DNA microarrays – future in oncology. *JCPCR* 2: 091–096.
- Król M, Pawłowski KM, Motyl T, 2009b. Mikromacierze DNA w onkologii weterynaryjnej [DNA microarrays in veterinary oncology]. *Medycyna Weterynaryjna* 65: 376–380.
- Król M, Pawłowski KM, Skierski J, Rao NAS, Hellmen E, Mol JA, Motyl T, 2009c. Transcriptomic profile of two canine cancer cell lines with different proliferative and anti-apoptotic potential. *J Physiol Pharmacol* 60: 95–106.
- Król M, Polańska J, Pawłowski KM, Turowski P, Skierski J, Majewska A, et al. 2010. Transcriptomic signature of cell lines isolated from canine mammary adenocarcinoma metastases to lungs. *J Appl Genet* 51: 37–50.
- Lindblad-Toh K, Wade CM, Mikkelsen TS, et al. 2005. Genome sequence, comparative analysis and haplotype structure of the domestic dog. *Nature* 438: 803–819.
- Macoska JA, 2002. The progressing clinical utility of DNA microarrays. *CA Cancer J Clin* 52: 50–59.
- Madej JA, Rotkiewicz T 2006. *Patologia ogólna zwierząt (General animal pathology)*. Olsztyn: Uniwersytet Warmińsko-Mazurski.
- Misdorp W, 2002. Tumors of the mammary gland. In: *Tumors in domestic animals*, 4th ed., Iowa State Press, Blackwell Publ. Comp. 589–602.
- Misher H, Lazareva-Ulitsky B, Loo R, Kejariwal A, Vandergriff J, Rabkin S, et al. 2005. The PANTHER database of protein families, subfamilies, functions and pathways. *Nucleic Acids Res* 33: 284–288.

- Oshlack A, Emsile D, Corcoran LM, Smyth GK, 2007. Normalization of boutique two-color microarrays with a high proportion of differentially expressed probes. *Genome Biol* 8:R2.
- Ougolkov AV, Billadeau DD, 2006. Targeting GSK-3: a promising approach for cancer therapy? *Future Oncol* 2: 91–100.
- Pawłowski KM, Król M, Majewska A, Badowska-Kozakiewicz A, Mol JA, Malicka E, Motyl T, 2009. Comparison of cellular and tissue transcriptomic profiles in canine mammary tumor. *J Physiol Pharmacol* 60: 85–94.
- Ramaswamy S, Ross KN, Lander ES, Golub TR, 2002. A molecular signature of metastasis in primary solid tumors. *Nat Genet* 33: 49–54.
- Rao NAS, van Wolferen ME, Gracanin A, Bhatti SFM, Król M, Holstege FC, Mol JA, 2009. Gene expression profiles of progesterin-induced canine mammary hyperplasia and spontaneous mammary tumors. *J Physiol Pharmacol* 60: 73–84.
- Rao NAS, van Wolferen ME, van der Ham R, van Leenen D, Groot Koerkamp MJA, Holstege FCP, Mol JA, 2008. cDNA microarray profiles of canine mammary tumor cell lines reveal deregulated pathways pertaining to their phenotype. *Anim Genet* 39: 333–345.
- Rolny C, Capparuccia L, Casazza A, et al. 2008. The tumor suppressor semaphorin 3B triggers a prometastatic program mediated by interleukin 8 and the tumor microenvironment. *J Exp Med* 205: 1155–1171.
- Rutteman GR, Cornelisse CJ, Dijkshoorn NJ, Poortman J, Misdorp W, 1988. Flow cytometric analysis of DNA ploidy in canine mammary tumors. *Cancer Res* 48: 3411–3417.
- Sobczak-Filipiak M., Malicka E., 2005. Estrogen receptors in canine mammary gland tumours. *Pol J Vet Sci* 5: 1–5.
- Spee B., Jonkers MDB, Arends B, Rutteman GR, Rothuizen J., Penning LC, 2006. Specific down-regulation of XIAP with RNA interference enhances the sensitivity of canine tumor cell-lines to TRAIL and doxorubicin. *Mol Cancer* 5:34.
- Sterrenburg E, Turk R, Boer JM, van Ommen GB, den Dunnen JT, 2002. A common reference for cDNA microarray hybridizations. *Nucleic Acids Res* 30: 116.
- Suyama E, Wadowa R, Kaur K, et al. 2006. Identification of metastasis-related genes in a mouse model using a library of randomized ribozymes. *J Biol Chem* 281: 18264.
- Tusher VG, Tibshirani R, Chu G, 2001. Significance analysis of microarrays applied to the ionizing radiation response. *Proc Natl Acad Sci U S A* 98: 5116–5121.
- Wagner K, Hemminki K, Grzybowska E, Klaes R, Burwinkel B, Bugert P, et al. 2006. Polymorphisms in genes involved in GH1 release and their association with breast cancer risk. *Carcinogenesis* 27: 1867–1875.
- Veer LJ van 't, Dai H, Vijver MJ van de, He YD, Hart AA, Peterse HL, et al. 2002. Gene expression profiling predicts clinical outcome of breast cancer. *Nature* 415: 530–536.